Demagnetization Analysis of Mechanical Manipulation on Permanent Magnets

Marcelo Ribeiro, Leonardo Martins, Michael Ortner
Microsystem Technologies
CTR – Carinthian Tech Research
Villach, Austria
marcelo.ribeiro@ctr.at

***Abstract* – This work comprises a study on the influences of mechanical manipulation on the magnetic field of permanent magnets. The focus lies in an analysis of resulting volume-demagnetization effects. This is brought out in a comparison between simulation results, based on analytical shape variation, and a magnetic position experiment. In the study, it was found that the datasheet remanence field values are overestimated by more than 30 % by the manufacturer, and that magnetic field attenuation resulting from demagnetization due to the mechanical manipulation is below 4 % for the chosen polymer bound Neodymium material.**

Keywords — magnetic sensing; magnetic simulations; mechanical manipulation; magnetic field shaping

I. Introduction and Motivation

Magnetic position and orientation detection systems typically feature a permanent magnet that moves relative to a magnetic sensor so that the mechanical motion can be calculated from the sensor output. Such systems are found in a wide range of industrial applications [1, 2], and can most of the time be realized with standard off-the-shelf permanent magnets. However, in many cases system integration requires custom-made magnets to fit the geometrical needs or to achieve desired field distributions [3]. The realization of such special forms, e.g. by injection mold technology, is uneconomical when only small numbers are needed, especially for fast integration and testing, it is straightforward to simply manipulate standard magnets mechanically. An open question is what consequences would such mechanical manipulations cause, keeping in mind that the manipulation of permanent magnets can result in mechanical stress and temperature variations throughout the sample and permanent magnetism is a volatile phenomenon affected by either of these.

It is the aim of this work to understand the influences of mechanical manipulation on magnetization and, as a result, on the magnetic field of permanent magnets. Potential applications include:

- System integration: Change magnet dimensions and shape in order to physically integrate into an existing system.
- Field Shaping: By changing the geometric shape of a permanent magnet it is possible to shape its magnetic field in a desired way in order to fine tune a setup or realize complex magnetic maps.
- Cost efficiency: It is cheaper to mechanically manipulate permanent magnets than to produce special shapes in small batches.

This work is structured as follows: In section II the proposed method is discussed. Section III covers the magnetic position experiment, explaining in detail what tools were used for the mechanical manipulation of the magnets and how the geometric changes were performed. In section IV the simulation is discussed and compared to the experimental results. Finally, results and interpretations are reviewed in the conclusion in section V.

II. Proposed Solution and Methodology

As a result of the mechanical manipulation, demagnetization effects are expected throughout the permanent magnet body. State of the art analysis tools like magnetic force microscopy [4] are limited to studying magnetic domains and surface effects. However, such an analysis is only of limited interest for this study as the magnetic field is generated by the sum of all volume elements of the permanent magnetic sample.

In this study, the analysis of the volume-demagnetization is performed by a measurement of the magnetic field in a defined region and by comparison to a simulation. In a first step, the simulation is calibrated by the measurement of the original magnet samples of homogeneous magnetization and known geometry. Then, the samples are mechanically manipulated in two defined subsequent steps. Each time the measurement is compared to the simulation of a similar geometric form to find discrepancies that hint at demagnetization within the samples.

III. Development & Experiment

A. Choice of magnet and material

It was chosen to work with a NeoAlphaMagnet NA022 from IBS Magnets (Fig. 1), a plastic bonded permanent magnet made of Neodymium-Iron-Boron (NdFeB) produced with a blend of magnetic powder mixed with an epoxy resin. This composite material is less brittle, thus allowing easier mechanic manipulation.

0-7695-6405-4/18/$31.00 ©2018 IEEE
DOI 10.1109/UKSim.2018.00041

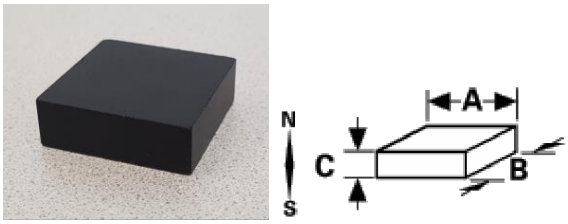

Figure 1. Permanent magnet used for the experiments

NdFeB is a state of the art material for permanent magnets with large coercivity (Hc) and, thus less prone to demagnetization, as well as large remanence (Br), which guarantees strong magnetic fields.

Below are the main datasheet specs of the chosen magnet:

- **Type:** NeoAlphaMagnet NA022
- **Br:** 700-800 mT
- **Hc-B:** 416-480 kA/m
- **Dimensions:** A=30 x B=30 x C=10 mm

The large magnet dimensions were chosen in order to facilitate the mechanical manipulation while relatively decreasing the errors due to tolerances.

B. Setup and tools

1) Simulations

In this paper, the magnetic fields are calculated by analytical means using solutions of permanent magnet problems [5, 6]. These solutions follow from directly solving Maxwell's equations for homogeneous magnetization distributions. Dynamic material properties that lead e.g. to demagnetization are not considered. For modern permanent magnetic materials, this is justified in a good approximation because of the large coercive fields and relative remanent permeabilities close to one, $\mu_r < 1.1$. Tests of the analytical formulas by FEM simulation showed that qualitative deviations are below 1% for the L/D ratio used in this work. However, the analytical models underestimate the remanence field in this setup by almost 6% as a result of homogeneous demagnetization effects.

Analytical models are much faster than FEM calculations, so that they can be used for field shaping and shape variation problems [7], which are critical for the optimization procedure used for analysis in this paper.

2) Experimental setup

The experiments were performed with a TLV493D, a 3D Hall sensor from Infineon, supported by a robot arm that can precisely carry and place the magnet in the vicinities of the sensor commanded by the in-house developed RAMSRS (Robot-Aided Magnetic Sensors Readout Suit, [8]).

The main characteristics of the experimental setup are as follows:

- **Sensor:** Infineon TLV493D (Fig. 2 (a))
- **Operation range:** ±200mT (±130mT)
- **Resolution:** 12-bit per field component (XYZ)
- **Robot Arm:** EPSON E2S SCARA (Fig. 2 (b))
- **Control and readout software:** RAMSRS

Figure 2. (a) 3D magnetic sensor; (b) Robot arm

3) Mechanical manipulation tools

A milling machine was used to perform the drills and cuts, while a sandpaper machine was used for final polish. Care was taken when performing all the manipulations to decrease heat generation, impacts and vibrations. The tools used for the mechanical manipulations can be found in Fig. 3 and 4.

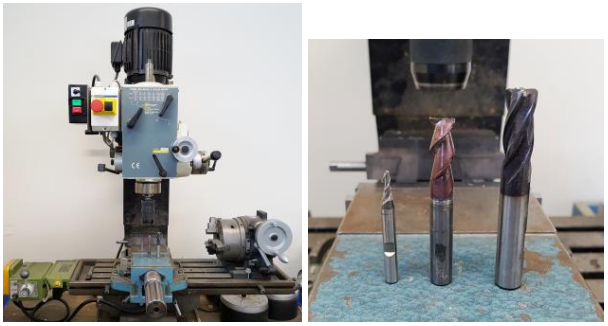
Figure 3. (a) Milling machine used to manipulate the magnets; (b) Specific tools used to perform the drills and cuts

Figure 4. Sandpaper machine used for final polishing of the magnets

C. Magnet Manipulations

It was chosen to perform simple geometric changes on the magnets in order to facilitate the simulation and allow the use of the tools available in house for the mechanical manipulation, taking care to reduce mechanical stress and therefore minimizing demagnetization issues. The sketch of the planned geometric changes can be found in Fig. 5.

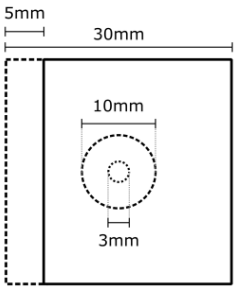

Figure 5. Sketch of the planned mechanical manipulations

Those geometric changes were performed on two magnets and consisted of drills, cuts and sanding to achieve the desired shapes. They were executed in a step-by-step scheme, using different sequences of manipulation for comparison. The pictures of the sequential mechanical manipulations of two sample magnets are shown in Fig. 6.

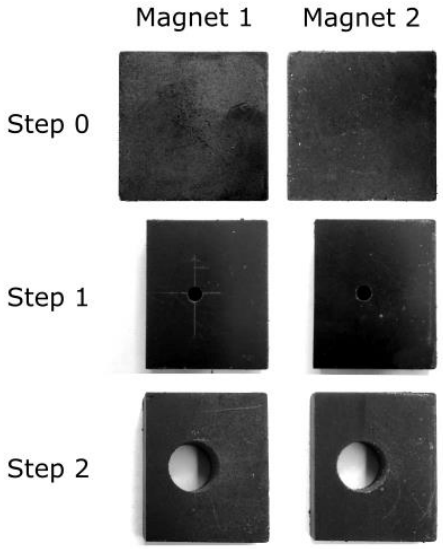

Figure 6. Mechanical manipulation steps of two sample magnets

The columns show the two manipulated magnets, while the rows show the mechanical manipulations, one step after the other:

- **Step 0:** untouched magnets
- **Step 1:** 3mm diameter drill and 5mm cut
- **Step 2:** larger drill (10mm diameter)

After finishing the manipulations, the dimensions were controlled to check the errors due to mechanical tolerances. The measured values can be found in Fig. 7.

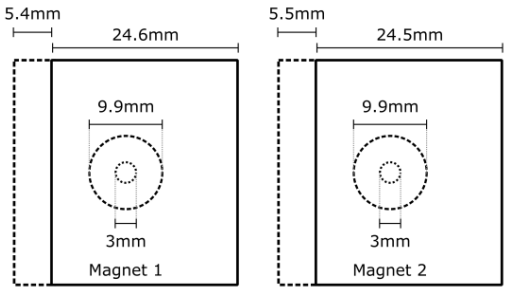

Figure 7. Sketch of the measured dimensions after the manipulations

D. *Experiment Layout*

1) *Measurement description*

The measurements were performed by fixating the sensor on a static sensor holder and the magnets on a magnet holder attached to the RAMSRS. Controlled by the RAMSRS, the robot arm positioned the magnets over the sensor at a fixed air-gap (distance between sensor and magnet) of 7.2 mm and moved the magnet in an XY plane of 50x50mm, centered over the sensitive elements inside the sensor's package.

The air-gap was selected magnetically for optimal sensor performance: a certain magnetic field value was chosen for the B_z component (60mT) and the distance between magnet and sensor was varied with the RAMSRS until this value was reached. The distance in mm was then measured from the surface of the magnet to the position of the sensitive element inside the sensor (according to the datasheet).

The boundaries of the XY plane were defined due to the magnet's size: considering the center of the sensor and magnet to be the XY zero point, at the lines of the boundaries (±25mm XY) the body of the magnet stays at least 10mm away from the sensor, which is enough for a good representation of the field intensities measured by the sensor on the plane, thus allowing easier analysis when the magnets are manipulated. Fig. 8 shows a sketch of the movement ranges and boundaries.

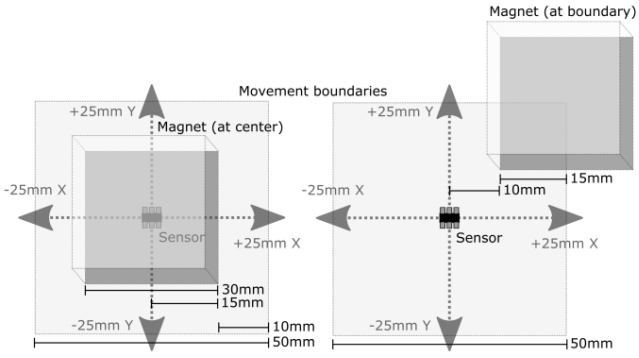

Figure 8. (a) Sketch of the experiment layout with the magnet centered over the sensor; (b) Representation of the magnet positioned over one of the extremities of the boundaries

After defining the air-gap and movement ranges, the system was magnetically calibrated by fine positioning the

magnet in a point where the B_z component was at its maximum (60mT) and B_x and B_y were zero.

After calibration, the measurements were started sweeping the whole 50x50mm plane over the sensor with a 500µm fine grid and collecting 50 sensor readouts at each step, this means 101 X repositions times 101 Y repositions times 50 sensor readouts, resulting in ~510k data samples for each of the measurements.

The largest discrepancies result from: soldering the sensor onto the PCB and placement of the latter on the sensor holder (±0.5mm displacement, ±3° sensor rotation), tolerances of the sensitive elements inside the chip package (0.1mm displacement, unknown rotation), tolerances of the magnet holder and positioning the magnet inside the holder (0.5mm displacement, ±1° magnet rotation). Most of these influences are eliminated by the magnetic calibration procedure. The total estimated precision is less than ±1mm relative displacement and ±3° relative rotation.

2) Experimental raw data

The experimental results are shown in Fig. 9 (a)-(f). The figures cover the sensor output of all three components of the field of both magnet samples for all three different steps of mechanical manipulation in the scanned region.

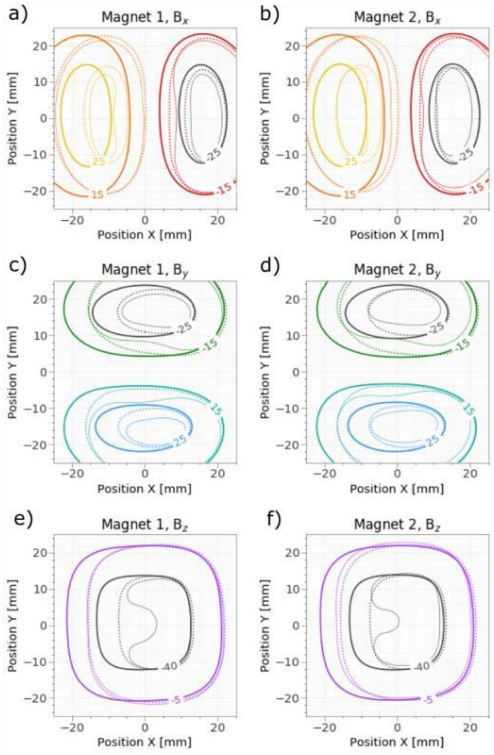

Figure 9. Raw output data of all experiments in comparison

Solid contours represent the fields from the original samples. Notice the high level of symmetry in all three components. Dotted contours represent the fields after the first manipulation step where one side was cut off and a small hole was drilled through the center. Finally, the solid thin contours represent the measurement from the last step where a large hole is drilled in the center. In both cases the contours adequately reflect the performed manipulations. Observable small differences between the two samples are expected as a result of imperfect mechanical manipulation and unaligned measurements.

IV. Analysis & Results

A. Analytical shape variation

In this work, analytical shape variation is used to calibrate and adjust the simulation. This technique is described in [7] and refers to performing geometric and material parameter variations of a permanent magnet and using analytical solutions of the magnetic field, to perform numerical tasks. The speed of the analytical solution makes it possible to use sophisticated multi-dimensional optimization algorithms. This was demonstrated in [9] where the field component of a magnet assembly was linearized in a designated region with help of a global differential evolution algorithm. In [7], the same technique was applied to determine experimental faults in a linear position experiment.

In this work, shape variation is used to calibrate the experiment and to find discrepancies between predictions by the simulation and the measured geometric dimensions outlined in Fig. 7. To that end, the measured fields are compared to the simulated ones. Then the chosen parameters are locally varied about their expected values until a minimal discrepancy between simulation and experiment is achieved. The employed numerical method uses quasi-newton based line search algorithms in an iterative scheme that picks the optimal search direction in each step. The iteration is stopped when the quadratic mean deviation shows improvements of below 1% in three subsequent steps.

For each simulation, the variation parameters are picked in accordance with the desired analysis. However, there is always a similar basis set that accounts for usual discrepancies in position experiments [7]. This set includes three angles of orientation of the magnet, magnet displacements in all three directions, as well as three angles of orientation of the sensor. These parameter variations account for the mechanical tolerances involved with assembling the system described in section III-C.

Multivariate optimization algorithms tend to overfit when the number of variables becomes too large. In this study, this danger is avoided by comparing a large region with respective 101x101 measurements. All variation parameters are carefully checked to remain within allowed tolerances estimated in the experimental setup. In the algorithm, these boundaries are not enforced.

B. Simulation Calibration

In the first step, the simulation is tested and calibrated by comparison to the measurements of the untouched magnet samples, where no demagnetization effects are expected. The shape variation is performed with respect to the basic parameter set described previously, as well as the remanence field.

The result of the simulation is shown in Fig. 10. The contour lines of the experiment (solid) and the simulation (dashed) show the good qualitative fit. In the background the colored contour plot shows the deviation between simulation and experiment in percent of the maximal field amplitude. One percent corresponds to approximately 0.6mT. The deviations for the two magnets are below 4% and 2% respectively which gives an interpretation limit of this simulation method.

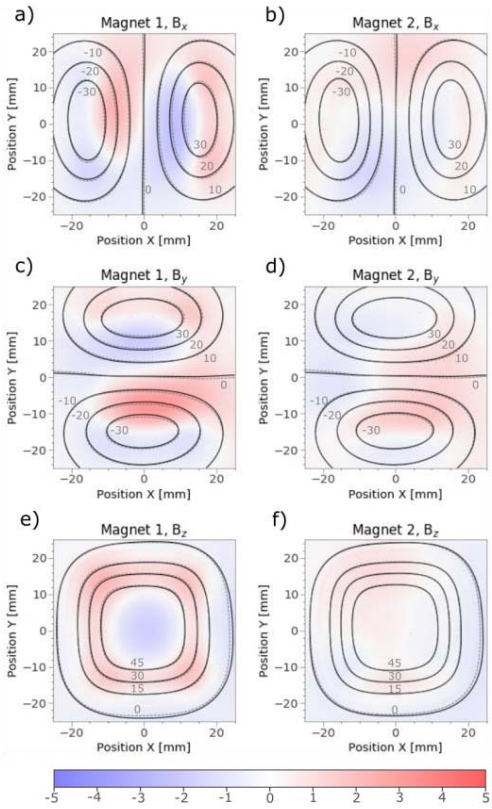

Figure 10. Magnetic field components of the two original magnet samples

For the nine base parameters, all displacements are below 1mm and rotations are below 1.8°, thus within acceptable experimental error bounds for both samples. The simulation estimates a remanence field of only ~433mT and ~428mT for the two samples. Including the 6% underestimation from the simulation these values are still more than 30% lower than the claimed material parameters from the manufacturer. Previous studies have detected similarly large deviations from datasheet values for different samples from other providers as well.

C. First Manipulation

In this step, the shape variation method is applied to determine position of the cut as well as the position of the small bore hole. Results based on the optimal simulation values are shown in Fig. 11.

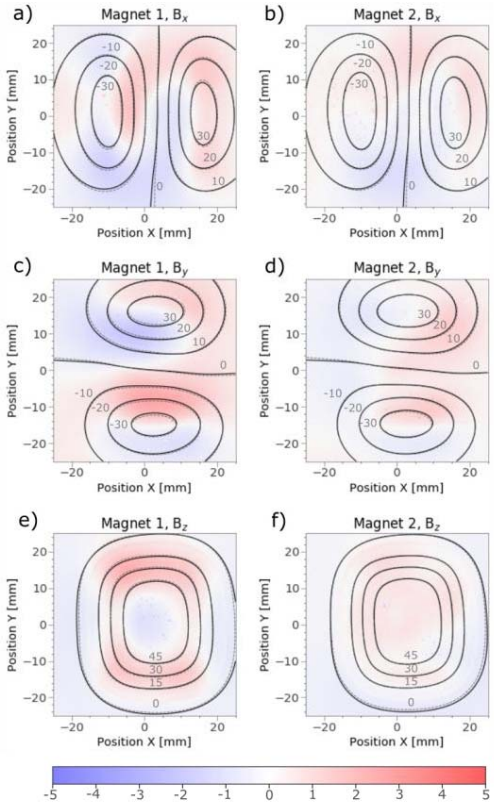

Figure 11. Magnetic field components of the two magnet samples after the first mechanical manipulation step

Solid and dashed contour lines show simulation and experimental results respectively. The colored contour shows the relative deviation between the two in percent of the maximal field amplitude. Deviations between experiment and simulation are below 3.5% and 2% for the two samples respectively. The base variation parameters are all within the acceptable 1mm or 2° deviation. Unfortunately, the small hole makes up only 2.3% of the total volume of the magnet and has such a small influence on the magnetic field that it is barely tractable and ignored by the optimization algorithm. The position of the cut, however, is estimated at 5.21 mm and 5.50mm for the two samples which coincides well with the measured values in Fig. 7 within 4% and 2%. As the simulation result coincides with the measured geometric parameters, it can be assumed that, within the interpretation limit, the remaining material is not demagnetized.

D. Second Manipulation

Finally, in the last step the additional variation parameters are the position of the large bore hole as well as

its radius. Comparison between experiment and simulation are shown in Fig. 12.

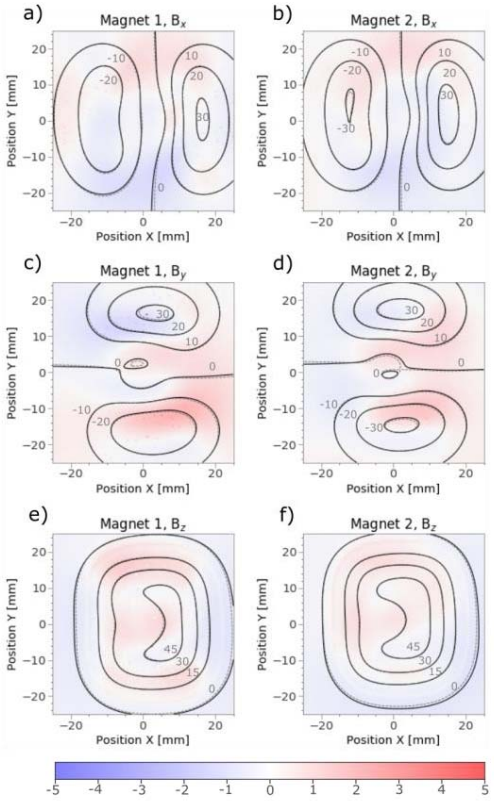

Figure 12. Magnetic field components of the two magnet samples after the second mechanical manipulation step

Solid and dashed contour lines show simulation and experimental results respectively. The colored contour shows the relative deviation between the two in percent of the maximal field amplitude. The deviations between simulation and experiment are below 3% and base variation parameters are again within acceptable ranges. The large bore hole changes the magnetic field visibly. The simulation estimates that the hole position deviates minimally from the XY origin (less than 100 µm). For hole diameters, 9.94 mm and 11.2 mm are estimated for sample 1 and 2 respectively. While the first estimate equals the measured value, the second one is off by more than 13% which is a strong indication that demagnetization took place in the drilling process around the bore hole. However, as this effect is only observed for a single sample, one must be careful with this interpretation.

V. Conclusion

This work introduces a procedure to determine demagnetization effects in permanent magnets that result from mechanical manipulation by milling and sanding. The proposed method searches for discrepancies between experimental and simulation data. It is tested on magnet samples of rectangular geometry that are mechanically manipulated in two steps. The simulations are based on an analytical shape variation model and deviate from experimental findings by less than 4% of the field amplitude.

The simulation model seems to be in good agreement with the measurements and is able to account for calibration errors that are difficult to control experimentally. Within the interpretation limit of the model, i.e. 4% variation of the magnetic field amplitude, possible demagnetization was only observed in a single case. This apparent high level of tolerance to stress and temperature seems to be a feature of the chosen material, thus supporting the proposed idea to mechanically manipulate off-the-shelf permanent magnets. Additionally, it was found that the remanence fields of the delivered samples were more than 30% below than claimed datasheet values.

Future studies will be conducted for larger sample numbers, different materials and at smaller airgaps to increase the resolution of the setup. However, this would require the use of different magnetic field sensors as the field amplitudes easily exceed specified sensor limits.

Acknowledgment

This project has been supported by the COMET K1 center ASSIC - Austrian Smart Systems Integration Research Center. The COMET - Competence Centers for Excellent Technologies - program is supported by BMVIT, BMWFW and the Austrian federal provinces of Carinthia and Styria.

References

[1] C. Treutler, “Magnetic sensors for automotive applications,” Sensors and Actuators A: Physical, vol. 91, no. 1, pp. 2–6, 2001.

[2] Sensing the World, Infineon Technologies AG, 04 2016.

[3] Huber, Christian, et al. "Topology optimized and 3D printed polymer-bonded permanent magnets for a predefined external field." Journal of Applied Physics 122.5, 2017: 053904

[4] U. Hartmann, Magnetic force microscopy. Annual review of materials science, 29(1), 1999, 53-87

[5] J. Camacho and V. Sosa, “Alternative method to calculate the magnetic field of permanent magnets with azimuthal symmetry,” Revista mexicana de fisica E, vol. 59, no. 1, pp. 8–17, 2013.

[6] H. L. Rakotoarison, J.-P. Yonnet, and B. Delinchant, “Using coulombian approach for modeling scalar potential and magnetic field of a permanent magnet with radial polarization,” IEEE Transactions on Magnetics, vol. 43, no. 4, pp. 1261–1264, 2007.

[7] M. Ortner, Application of 3D-printed magnets for magnetic position detection systems, IEEE SENSORS proceedings, 2017, 190-193

[8] M. Ribeiro, "Robot-Aided Magnetic Sensors Readout Suit," 9th International Conference on Sensing Technology (ICST), Auckland, 2015, pp. 706-710. doi: 10.1109/ICSensT.2015.7438488

[9] M. Ortner, Improving magnetic linear position measurement by field shaping, 9th International Conference on Sensing Technology (ICST), Auckland, 2015, pp.359-364